Journal of Organometallic Chemistry, 197 (1980) 169—180
Elsevier Sequoia S.A., Lausanne — Printed in The Netherlands

METAL—SILICON BONDED COMPOUNDS

XIV. THE ELECTRONIC SPECTRA OF SILICON—MERCURY DERIVATIVES

T.F. SCHAAF, A.K. HOVLAND, W.H. ILSLEY and J.P. OLIVER [*]

Department of Chemistry, Wayne State University, Detroit, Michigan 48202 (U.S.A.)

(Received December 20th, 1979)

Summary

The ultraviolet and visible spectra of compounds of the general formula $Hg(SiCl_{3-x}R_x)_2$ where R = Me, Ph are reported. In addition spectra have been obtained on the compounds $Hg(GeMe_3)_2$, $Hg[Si(SiMe_3)_3]_2$ and the cyclic compound $\overline{HgSi(Me_2)CH_2SiMe_2HgSiMe_2CH_2Si}Me_2$. In cyclohexane all compounds show three characteristic bands, two at ~4 eV and one at ~6 eV. Extended Hückel calculations have been used to obtain a qualitative energy level scheme and to make tentative assignments for the transitions. The 4 eV transitions have been assigned to transitions from the ground state, $^1A_1$, to be $^1B_1$ and $^1A_2$ states respectively and the 6 eV transition to a transition to an excited $^1A_1$ state. The orbitals involved are principally centered on the mercury atom with their energies perturbated by the attached silicon moieties.

Introduction

Main group metal—silicon derivatives are of interest since they provide a convenient route for the selective introduction of silyl groups into a variety of compounds. The initial preparation of these compounds has not yielded to many of the methods currently found useful for traditional organic synthesis of carbon—metal bonds, but one route, the displacement of a less active metal by a more active species has proven to be widely applicable. For this reason these derivatives are of major interest in the study of metal—silicon species.

A wide variety of these silyl—mercury compounds are highly colored ranging from pale yellow, through orange, red and green. In spite of this and their known photochemical decomposition, only very isolated reports of the electronic spectra of these species have been published and no systematic study of the Si—Hg—Si chromophore has been made [1]. In this paper we report the UV-visible absorption spectra in three solvents of eleven silicon—mercury compounds and one germanium—mercury compound.

To facilitate assignment of bands a simple energy level diagram was constructed based on extended Hückel calculations carried out on these systems. Use of this set of energy levels led to assignments which are consistent with the large substituent and solvent effects observed in the absorption spectra.

Experimental

Preparation of compounds. All compounds were prepared and characterized using standard high vacuum, Schlenk, and drybox techniques. The general approaches used for the synthesis of the bis(silyl)— and bis(germyl) mercury derivatives have been reported by others [2]. The specific details and methods used for the preparation of the individual compounds involved in this study have been previously cited [3]. The preparation of the mercurates has been discussed in an earlier publication [1], but can be most expeditiously effected by addition of the stoichiometric amounts of the mercury derivative, $Hg(SiMe_3)_2$ and the lithium derivative, $(LiSiMe_3)_6$ in cyclopentane or hexane. The compounds have been characterized by chemical analysis, ^1H NMR, and for $Li_2Hg(SiMe_3)_4$ by a single crystal X-ray structural determination [4].

Solvents were of commercial spectroquality or reagent grade dried over sodium/potassium alloy and degassed on the vacuum line prior to use. Solutions were prepared by volumetric techniques in an argon filled drybox, placed in quartz cells and closed with plugs. The plug and joint were tightly wrapped with Parafilm T to exclude air and water. The cells were then removed from the drybox and the UV visible spectra were obtained immediately. Repetitive scans showed no evidence of decomposition during the first half hour after removal from the drybox. UV visible spectra were obtained on a Cary 14 spectrometer. Samples were run against air and corrections to the absorbance were made from appropriate blanks.

Calculations. Extended Hückel (EH) molecular orbitals calculations were carried out in the manner first described by Hoffmann [5,6]. The coulomb integrals, H_{ij}, were set equal to valence orbital ionization potentials (VOIP) for the particular orbital in question [7,8]. The VIOP's used for mercury were those previously reported [9]. The wave functions for the Hg atom included d orbitals, but those for the Si atoms did not. The resonance integrals, H_{ij}, were evaluated using the Wolfsberg—Helmholz expression with $K = 1.75$ for both σ and π interactions [10]. The overlap integrals, S_{ij}, were calculated using atomic self-consistent field wave functions. For all atoms the double Σ functions of Clement [11] were employed.

Charges were iterated to self-consistency using a charge sensitivity factor [CONCH(I)] of 2.00 eV/electron for all VIOP's and the calculate the Coulomb integrals as expressed by the equation:

$$H_{ii}^{k} = H_{ii}^{0} - \mathrm{CONCH(I)}\,\Sigma^{k-1}(\mathrm{I}) + \frac{\Sigma k(\mathrm{I}) - \Sigma(k-1)(\mathrm{I})}{2}$$

Where $\Sigma k(\mathrm{I})$ is the charge on atom I at cycle k. The self-consistency criterion for charges was taken as a difference of 0.01 e or less between the initial and final atomic charges of any atom for a given cycle.

Extended Hückel calculations were carried out on Hg[SiCl$_3$]$_2$ in the linear D_{3d} and the bent C_{2v} and C_s configurations. In addition Hg[SiMeCl$_2$]$_2$, Hg[SiMe$_2$Cl]$_2$, Hg[SiMe$_3$]$_2$ and Hg[GeMe$_3$]$_2$ were treated in the bent C_{2v} configurations and in the linear C_{2h} configurations.

Extended Hückel calculations were similarly carried out on the two mercury anions Hg(SiH$_3$)$_3^-$ and Hg(SiH$_3$)$_4^{2-}$ which were taken as models for the Hg(SiMe$_3$)$_3^-$ and Hg(SiMe$_3$)$^{2-}$ anions of LiHg(SiMe$_3$)$_3$ and Li$_2$Hg(SiMe$_3$)$_4$, respectively. The Hg(SiH$_3$)$_3^-$ anion was treated only in the planar C_{3h} configuration and the Hg(SiH$_3$)$_4^{2-}$ anion was treated as being perfectly tetrahedral. The Hg—Si and Si—Si bond lengths were set at 2.500 Å [4,12] and 2.36 Å [13], respectively. The Si—C and Si—H distances were set at 1.88 Å [14] and 1.48 Å [14], respectively. The C—H distances were set at the standard 1.095 Å and the Si—Cl distances at 2.109 Å [12]. Hg—Ge and Ge—C distances were set at 2.56 Å * and 1.99 Å **, respectively.

Results

Table 1 lists the compounds run, solvents, peak positions and extinction coefficients. Figure 1 shows the spectrum of bis(dichloromethylsilyl)mercury in cyclohexane. This spectrum exhibits three peaks characteric of compounds with two silicons coordinated to mercury: an intense peak at about 215 nm labeled A; and two much weaker peaks at lower but variable energy labeled B and C. Peak B is generally five to ten times more intense than peak C. The very small peak at 258.5 nm was not observed in other solvents or compounds although in some instances fine structure was detected about this wavelength.

In the series Hg(SiMe$_{3-x}$Cl$_x$)$_2$ peaks B and C showed a large hypsochromic shift as chlorine atoms replaced methyl groups. Surprisingly the energy separation between peaks B and C remained virtually constant at 0.6 eV (~5 kK) (Fig. 2) as chlorine atoms replaced methyl groups while peak A showed a small bathochromic shift.

On changing the solvent from cyclohexane to THF large hypsochromic shifts were observed in the series Hg(SiMe$_{3-x}$Cl$_x$)$_2$, for the B and C peaks (Fig. 2). The size of this solvent shift increased as more chlorine atoms were substituted on silicon, but again the separation between the B and C peaks remained close to 0.6 eV. The A peak showed only small shifts, this time hypsochromic.

Substitution of phenyl groups to yield the series of methylphenylsilyl derivatives lead to relatively small changes upon addition of the phenyl group for bands B and C while band A moved substantially to lower energy on introduction of the phenyl group and continued to have a bathochromic shift with addition of more phenyl substituents. The spectrum of Hg[Si(SiMe$_3$)$_3$]$_2$, in addition to showing a large bathochromic shift for the high energy band, also shows

---

* Sum of the covalent radius of Ge (1.22 Å) and the effective radius of Hg obtained from the Hg—Si derivatives (1.34 Å).

** Sum of the covalent radii of Ge (1.22 Å) and C (0.77 Å).

TABLE 1

A LIST OF THE MAJOR ABSORPTION MAXIMA AND EXTINCTION COEFFICIENTS FOR SILYL— AND GERMYL—MERCURY COMPOUNDS OBTAINED IN CYCLOHEXANE, THF AND Et_3N

Compound	Solvent	C		B		A	
		Å	ε	Å	ε	Å	ε
$Hg(SiMe_3)_2$	C_6H_{10}	3900	1.1×10^2	3280	3.7×10^2	2142	2.6×10^4
	THF	3700	7.6×10^1	3125	2.9×10^2	2125	2.2×10^4
	Et_3N	3860	8.7×10^1	3310	2.8×10^2	(obscured)	
$Hg(SiMeCl_2)_2$	C_6H_{10}	3308	8.4×10^1	2870	3.7×10^2	2175	2.2×10^4
	THF	2950	5.0×10^1	2550	7.0×10^2	2155	1.8×10^4
$Hg(SiMe_2Cl)_2$	C_6H_{10}	3560	1.6×10^2	3100	6.2×10^2	2120	5.5×10^4
	THF	3200	1.6×10^2	2740	4.4×10^2	2135	2.2×10^4
$Hg(SiCl_3)_2$	C_6H_{10}	3100	1.4×10^2	2660	1.1×10^3	2180	1.8×10^4
	THF	2700	1.3×10^2	2400	1.7×10^3	2150	8.7×10^3
$Hg[Si(SiMe_3)_3]_2$	C_6H_{10}	3900	2.3×10^2	3415	7.6×10^2	2050	1.0×10^5
				(2750	1.4×10^4)		
				(2580	2.5×10^4)		
				(2400	3.0×10^4)		
	THF	3900	1.8×10^2	3410	7.2×10^2	(out of range)	
				(2775	7.6×10^3)		
				(2510	2.6×10^4)		
$Hg(GeMe_3)_2$	C_6H_{10}	3640	1.8×10^2	3215	6.0×10^2	2300	4.6×10^4
	THF	2550	1.2×10^2	2955	5.2×10^2	2275	4.0×10^4
	Et_3N	3640	1.9×10^2	3180	5.5×10^2	(obscured)	
$Hg(SiMe_2Ph)_2$	C_6H_{10}	3870	1.8×10^2	3300	9.8×10^2	2650	9.0×10^3
$Hg(SiMePh_2)_2$	C_6H_{10}	3795	1.2×10^2	3250	1.7×10^3	2740	1.4×10^4
$Hg(SiPh_3)_2$	C_6H_{10}	3850		3300		2850	
$Hg_2Si_4C_{10}H_{28}$	C_6H_{10}		(4350	1.3×10^2)			
			(3840	6.3×10^2)			

several additional transitions discussed below. The B and C bands appear at about the same energies of those in $Hg(SiMe_3)_2$.

The ring compound $\overline{HgSi(Me_2)CH_2Si(Me_2)HgSi(Me_2)CH_2Si}(Me_2)$ (I) gave two broad bands at 435 and 384 nm with relatively low extinction coefficients of 1.3×10^2 and 6.3×10^2 respectively as well as several low intensity bands, (i.e. $\epsilon < 100$), at 290 and in the 255—275 nm region. Further there was large end absorption at ~190 nm. In triethylamine the spectrum was essentially unchanged but in THF no resolvable bands were observed in the 430 nm region, while a band at 374 nm remained and a new band with $\epsilon \sim 1.1 \times 10^4$ appeared at 217.5 nm.

The final sequence of compounds investigated were the lithium silylmercurates. $LiHg(SiMe_3)_3$ gave a single band at 513.0 nm with $\epsilon = 1.8 \times 10^2$ and end absorption in a THF solution and $Li_2Hg(SiMe_3)_4$ which showed only end absorption with several weak shoulders in the region of 202.5, 207.5 and 215.0 nm. These data show several clearly discernable trends which must be accounted for if the assignments are properly made.

In order to facilitate the assignment of the observed transition energies, extended Hückel (EH) molecular orbital calculations were carried out, on the

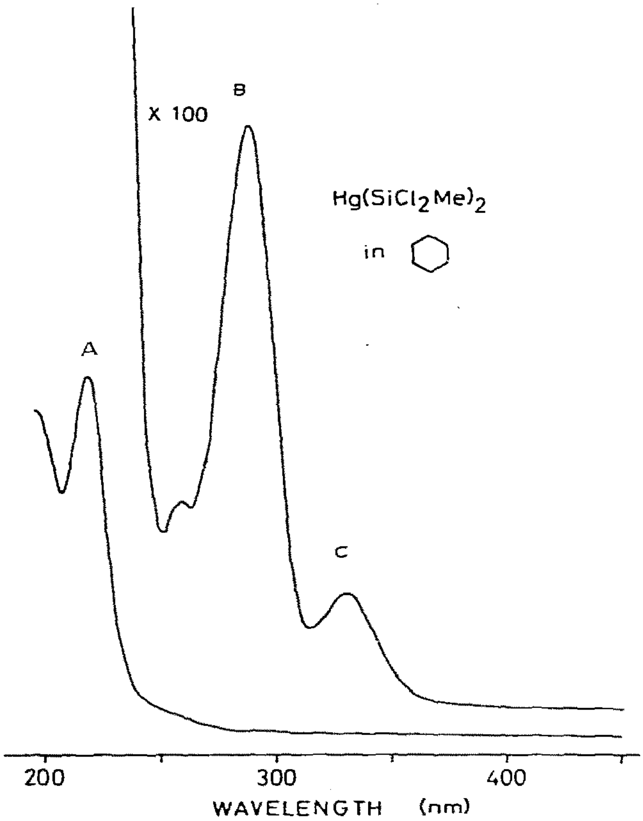

Fig. 1. The UV spectrum of $Hg(SiMeCl_2)_2$ obtained in cyclohexane solvent.

compounds with the general formula $Hg(SiMe_{3-x}Cl_x)_2$. In the application of these calculations, two distinctly different configurations of each of the molecules were considered. The first was a configuration in which each molecule was considered to possess a linear Si—Hg—Si framework and the second, the configuration in which each molecule was considered to have a bent Si—Hg—Si framework. Point group assignments were made for each compound in both configurations of the Si—Hg—Si framework on the assumption that free rotation about the Si—Hg and the Si—C bands occurred. The possible point groups for each of the molecules are summarized in Table 2.

Figure 3 shows qualitative energy level schemes which are predicted on the basis of the extended Hückel calculations for bis(trichlorosilyl)mercury in the linear D_{3d} configuration and in the bent C_{2v} and C_s configurations. The figure summarizes a number of important considerations which we shall now examine. Let us first consider the energy level scheme for $Hg(SiCl_3)_2$ in the linear D_{3d} configuration. Figure 3 shows the two highest occupied and four lowest unoccupied molecular orbitals. Pictorial representations of the orbitals are presented at the left of the figure along with the coefficients associated with the atomic orbitals contributing to the molecular orbital. In order of increasing energy the orbitals are (i) a σ bonding MO which is predominantly

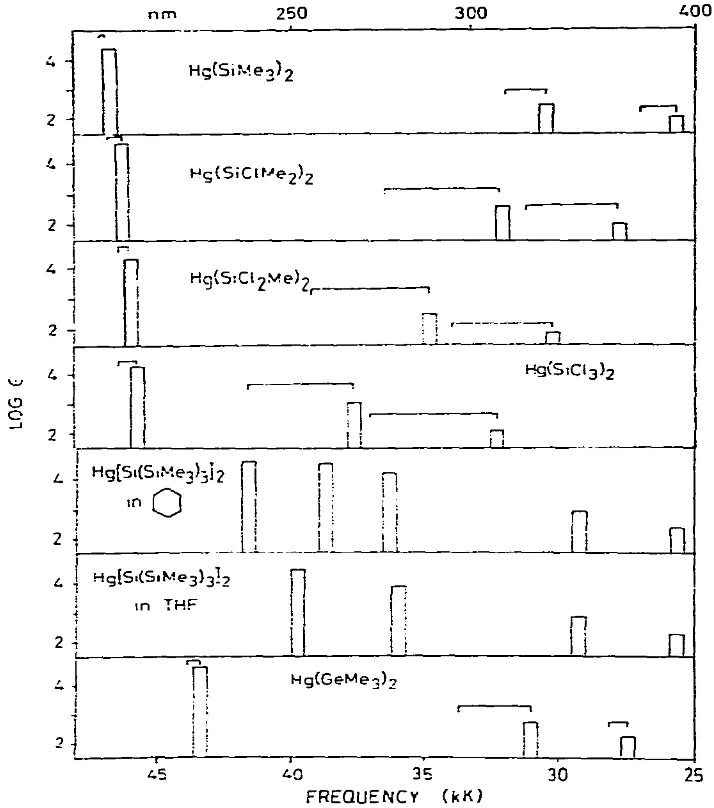

Fig. 2. A plot of the principal absorption bands of a series of silyl— and germylmercury derivatives showing the hypsochromic shift which occurs when the solvent is changed from cyclohexane to THF.

mercury 6*s* in character with minor contributions for the silicon p_x orbitals, (ii) a σ bonding orbital which is primarily mercury $6p_x$ in character with minor contributions from the silicon p_x atomic orbitals, (iii) two degenerate unoccupied nonbonding mercury p_y and p_z orbitals, and (iv) two anti-bonding orbitals with contributions from both silicon and mercury.

TABLE 2

POSSIBLE POINT GROUPS ASSUMING FREE ROTATION ABOUT THE Si—Hg AND Si—C BONDS FOR $Hg(SiMe_nCl_{3-n})_2$ DERIVATIVES

Compound	Linear	Bent
$Hg(SiMe_3)_2$	D_{3d}, D_{3h}, D_3 C_i, C_2, C_1 C_{2v}, C_{2h}, C_s	C_{2v}, C_s, C_1, C_2
$Hg(SiMe_2Cl)_2$	C_{2v}, C_{2h}, C_2 C_1, C_i, C_s	C_{2v}, C_s, C_1, C_2
$Hg(SiMeCl_2)_2$	C_{2h}, C_s, C_1 C_{2v}, C_i, C_2	C_{2v}, C_s, C_1, C_2
$Hg(SiCl_3)_2$	D_{3d}, D_{3h}, D_3	C_{2v}, C_s, C_1, C_2

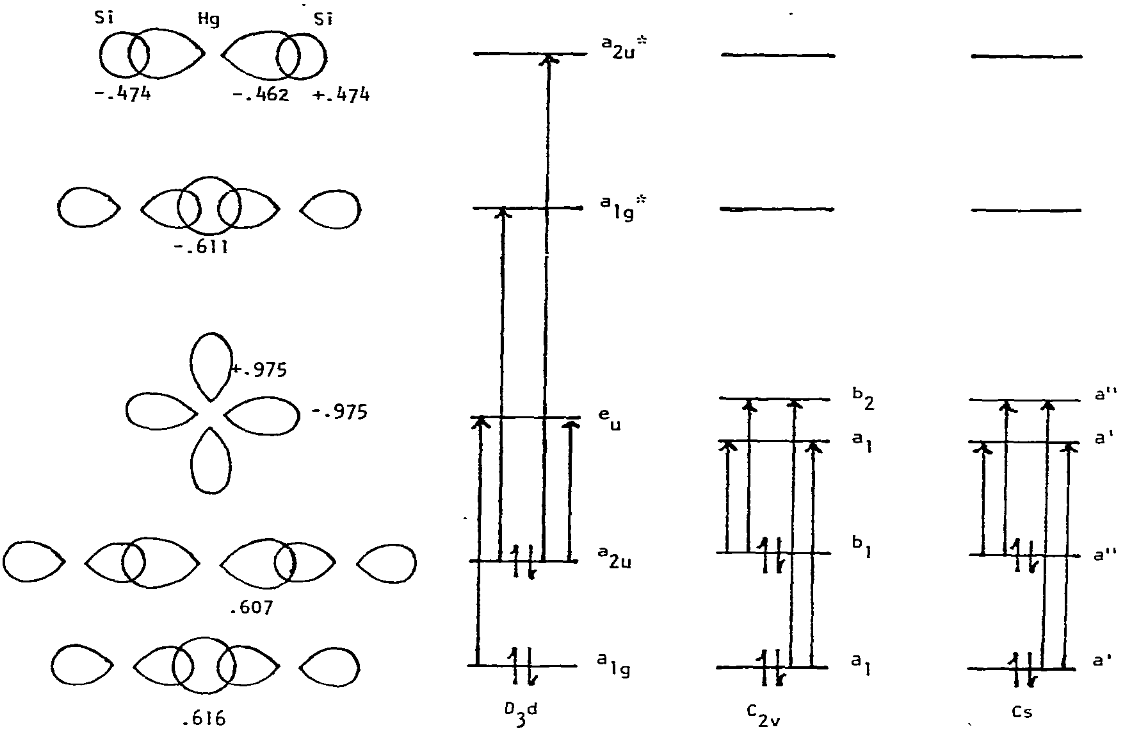

Fig. 3. Qualitative energy level diagrams for $Hg(SiCl_3)_2$ in D_{3d}, C_{2v}, and C_s symmetry. The diagrams at the left represent the principle atomic orbitals forming the energy level and coefficients of these orbitals.

In D_{3d} symmetry three transitions involving these orbitals are allowed, $a_{2u} \leftarrow a_{1g}{}^{*1}$, $a_{2u} \leftarrow a_{2u}{}^{*2}$, $a_{1g} \leftarrow e_u$ and one is forbidden $a_{2u} \leftarrow e_u$. The energies predicted from the EH calculations for the transitions are 15.4 eV, 11.9 eV, 6.09 eV and 3.53 eV, respectively. Clearly the two transitions involving the antibonding orbitals need not be considered further because of the extremely high energy involved. The remaining transitions have predicted energies that are good approximations of those observed (see Table 3). The transition at 6.09 eV

TABLE 3

A COMPARISON OF OBSERVED AND CALCULATED TRANSITION ENERGIES FOR SELECTED SILYL— AND GERMYL—MERCURY DERIVATIVES HAVING C_{2v} SYMMETRY

Compound	Band C		Band B		Band A	
	calcd.	obs.	calcd.	obs.	calcd.	obs.
$Hg(SiMe_3)_2$	3.54	3.18	3.63	3.78	5.76	5.79
$Hg(SiMe_2Cl)_2$	3.33	3.48	3.51	4.00	5.39	5.85
$Hg(SiMeCl_2)_2$	3.31	3.75	3.38	4.32	5.49	5.70
$Hg(SiCl_3)_2$	3.39	4.00	3.49	4.66	6.00	5.69
$Hg(GeMe_3)_2$	3.61	3.41	3.72	3.86	5.82	5.39
$Hg[Si(SiH_3)_3]_2$ [a]	3.40	3.18	3.50	3.63	6.35	6.05

[a] The observed energies are those for $Hg[Si(SiMe_3)_3]_2$.

corresponds to the high energy band which is observed in the 5—6 eV range for all of the compounds studied. The forbidden low energy band is also in the range with observed values ranging from 3—4.5 eV. The fact that two bands are observed in this low energy region may be accounted for in either of two ways; one might invoke spin-orbit coupling or alternatively one may consider other possible symmetries which are readily accessible through rotation or vibration of the $Hg(SiCl_3)_2$ molecule and which are inherent in the less symmetric systems. These are summarized in Table 2 and the change in energy states is shown in Fig. 3 for both C_{2v} and C_s symmetry. The e_u orbitals split as a result of the decrease in symmetry. In C_{2v} symmetry the $a_1 \leftarrow a_1$, $a_1 \leftarrow b_2$ and $b_1 \leftarrow a_1$ transitions become allowed while the $b_1 \leftarrow b_2$ transition remains symmetry forbidden. In C_s symmetry all of the transitions become symmetry allowed. Examination of Table 2 and Fig. 3 suggests four possible transitions, however only three are observed. Examination of the energy level diagram and the data in Table 1 showing the transitions suggest that the fourth high energy band should occur at approximately 0.6 eV above the A band (the difference between the B and C bands corresponds to the separation of the a and a'' orbitals, in C_s symmetry) or at 6 or more eV, which is at the cut off of the instrument. Thus it would appear that the transitions for the linear silyl—mercury derivatives are primarily centered on the mercury atom and are of the $\sigma \leftarrow n$ type. The non-bonding orbitals in this model are the p_y and p_z orbitals of mercury.

Supporting evidence for this energy scheme comes from the observed solvent effect. When the solvent is changed from a non-interacting solvent, cyclohexane, to a strongly interacting solvent, THF, for the series $Hg(SiMe_nCl_{3-n})$ ($n = 0$—3) as seen in Fig. 2, the B and C band shift to higher energy by an equivalent amount in each compound. This would be expected with interaction of THF with the vacant p_y and p_z orbitals, Fig. 6. Further, there is little change in the A band which can readily be accounted for since it corresponds to a transition from an orbital primarily of mercury 6s character to the mercury p orbitals both of which will be raised in energy on interaction with THF.

The single example of a germanium compound, $Hg(GeMe_3)_2$, appears to fall in the same group with similar transitions and solvent dependence.

To extend the calculation to more complex derivatives, such as $Hg[Si(SiMe_3)_3]_2$ and the anionic species $Hg(SiMe_3)_3^-$ and $Hg(SiMe_3)_4^{2-}$ is non trivial because of the number of orbitals involved. Therefore to reduce this problem, model calculations were carried out on the corresponding hydrogen derivatives, i.e. the SiH_3 derivatives.

The energy level scheme calculated for $Hg[Si(SiH_3)_3]_2$ in C_{2v} symmetry is shown in Fig. 4. From this figure we note that transitions analogous to those predicted for the series $Hg(SiMe_{3-x}Cl_x)_2$ are again predicted for $Hg[Si(SiMe_3)_3]_2$. These are the transitions 1, 2 and 3, respectively. There are, in addition, at least four other transitions predicted at about 5 eV's. Examination of Table 1 reveals that there are, indeed, three resolvable transitions observed at the predicted energy for $Hg[Si(SiMe_3)_3]_2$. The actual spectrum, however, shows a very broad and rather unresolved band at approximately 5 eV so it is not surprising that we are not able to assign a fourth transition in this region as predicted by the Extended Hückel calculations. These additional bands arise from

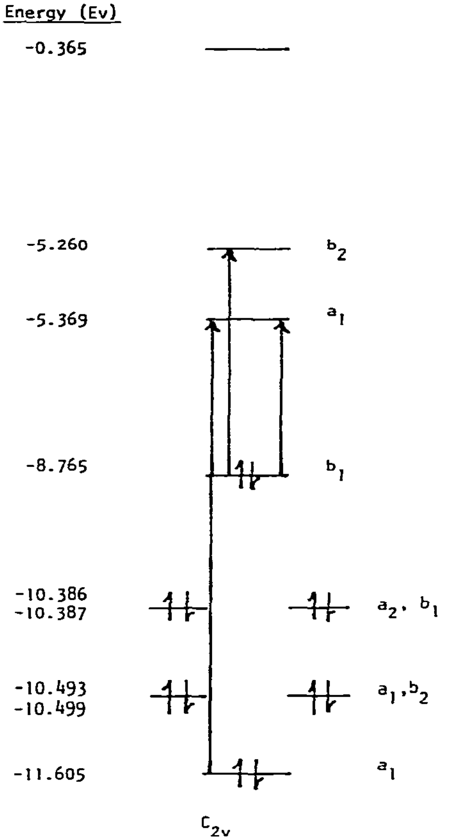

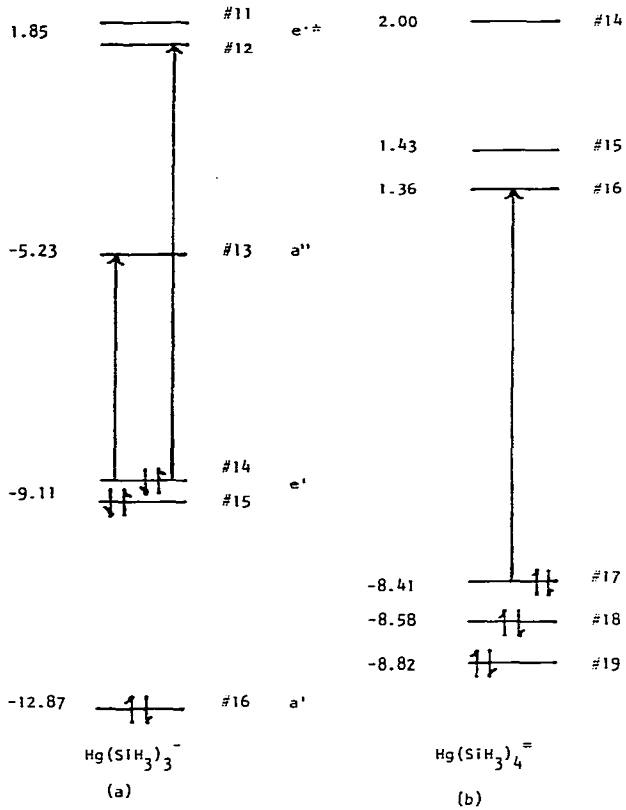

Fig. 4. An energy level diagram calculated for $Hg(Si(SiH_3)_3)_2$ having idealized C_{2v} symmetry.

Fig. 5. An energy level diagrams calculated for the $Hg(SiH_3)_3^-$ and $Hg(SiH_3)_4^{2-}$ anions.

transitions from orbitals centered mainly on the silicons to the non-bonding *p* orbitals on mercury. Extended Hückel calculations also were carried out on the $Hg(SiH_3)_3^-$ and $Hg(SiH_3)_4^{2-}$ anions in order to see if the calculations would predict the experimental results obtained for the compounds $LiHg(SiMe_3)_3 \cdot$ 3 DME and $Li_2Hg(SiMe_3)_4$. Figure 5 shows a summary of the energy level schemes obtained. We have presented in Fig. 5 the three highest occupied and the three lowest unoccupied orbitals. Orbital 16 (a' symmetry) is a σ-bonding orbital which is predominantly mercury 6*s* with minor contributions from the silicon p_x and p_y orbitals as defined in the calculation. Orbitals 14 and 15 are a set of degenerate σ-bonding orbitals which are delocalized over the mercury and two of the silicon atoms. These orbitals are composed of approximately equivalent orbital contributions from both the mercury p_x and p_y atomic orbitals and the p_x orbital of one silicon and the p_y orbital of the second silicon. Orbital 13 is the non-bonding p_z orbital of mercury and the e'^* orbitals 11 and 12 are the anti-bonding orbitals corresponding to the bonding e' orbitals 14 and 15. Examination of Fig. 5 reveals that for the $Hg(SiH_3)_3^-$ the two lowest energy transitions are the $e' \leftarrow a''$ and the $e'^* \leftarrow e'$ transitions. The $e'^* \leftarrow$

e' transition has a predicted energy of 10.96 eV. This transition is too high in energy to be observed. The $e' \leftarrow a''$ transition with a predicted energy of 3.88 eV is of low enough energy to be observed under the conditions of this study. It will be observed that the predicted energy of 3.88 eV is far greater than the observed transition energy of 2.46 eV for $LiHg(SiMe_3)_3 \cdot 3$ DME. This can be attributed to at least two factors. First and foremost, due to the nature of the calculation, the predicted energies cannot be expected to be very good. In addition, since the calculations were carried out on $Hg(SiH_3)_3^-$ instead of $Hg(SiMe_3)_3^-$ we cannot expect the calculated energies to be a very good approximation to that observed for the $Hg(SiMe_3)_3^-$ anion. We are also unable to predict the effect that solvent and substitution of methyl groups for hydrogens on $Hg(SiH_3)_3^-$ will have on the transition energy. The important point here is that in agreement with the experimental observations, only one transition is predicted for the tris-anion. In Fig. 5b we have again presented only the three highest occupied and three lowest unoccupied orbitals for the $Hg(SiH_3)_4^{2-}$ anion. For this anion the lowest energy transition is predicted to have an energy of 9.78 eV, this is far too high in energy to be observed under the conditions of this study. Consistent, therefore, with the experimental observations, th calculation predicts that there should be no observable transition. Further-

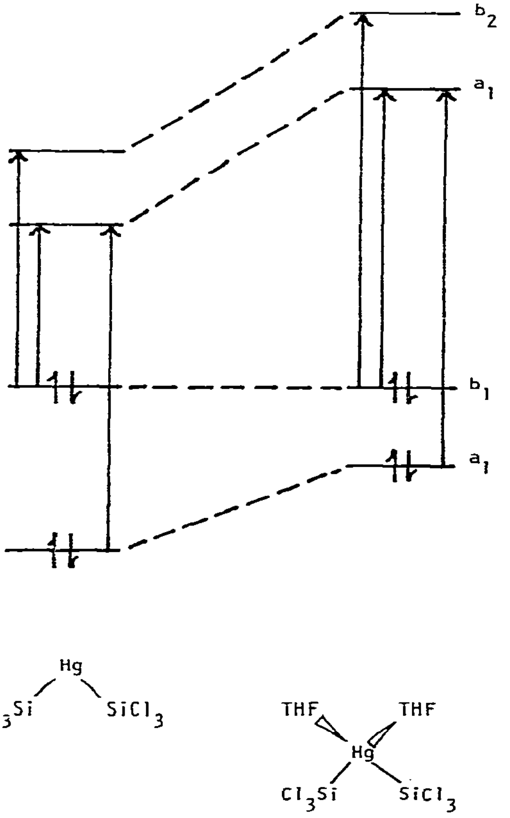

Fig. 6. The affect of THF coordination on the energy level of $Hg(SiCl_3)_2$ assuming the C_{2v} configuration which leads to the hysochromic shift of the band C bands.

more, they suggest that the main chromophore in these compounds is the mercury itself and that we are observing transition between the filled bonding *s* (mainly) and *p* (mainly) orbitals on mercury to the unoccupied non-bonding orbitals on mercury. For the compounds of general formula $Hg(SiMe_{3-x}Cl_x)_2$ the observed transitions correspond to the $b_1 \leftarrow a_1$ (C transition), $b_1 \leftarrow b_2$ (B transition), allowed through vibronic coupling and the $a_1 \leftarrow a_1$ (A transition).

Let us now consider the experimentally observed trends in light of the qualitative energy scheme presented above. Close examination of Table 1 reveals that in going from a noncoordinating solvent (cyclohexane) to a highly coordinating solvent such as THF there is a shift of all three transitions to higher energy with the exception of band A on the spectrum of $Hg(SiMe_2Cl)_2$. As we have pointed out above, the main chromophore in these compounds is the mercury atom, and the observed bands are a result of transitions between the filled *s* and p_x to the nonbonding p_z and p_y orbitals on mercury. Assuming this to be the case one can explain the observed shifts to higher energies as being a direct result of coordination of the THF molecules with the mercury. Such coordination would result in an increase in the energy of the nonbonding *p* orbitals thereby shifting the transitions to higher energy. It is interesting to note that even though there is a shift of the B and C transitions to higher energy the energy difference between the two transitions remains approximately constant at about 0.6 eV's. This is consistent with the postulated coordination of the THF molecules to the mercury atom. The A band is also shifted to higher energy but by a somewhat lesser amount than the B and C bands. This shift can be explained if one postulates that since the a_1 orbital is predominantly Hg(*s*) in character, due to the coordination with THF this level is raised somewhat higher in energy relative to the unoccupied *p* orbitals. This would explain the smaller shift for this transition relative to the B and C bands, see Fig. 6.

Acknowledgements

This work was supported in part by the National Science Foundation grants CHE-75-17217 and CHE-79-13182. William H. Ilsley was a Lubrizol Foundation Fellow (1977—78).

References

1 T.F. Schaaf and J.P. Oliver, J. Amer. Chem. Soc., 91 (1969) 4327.

2 C. Eaborn, W.A. Dutton, F. Glocking and K.A. Hooton, J. Organometal. Chem., 9 (1967) 175; W.P. Neumann and U. Blankat, Angew. Chem., Int. edit., 8 (1969) 611; C. Eaborn, R.A. Jackson and R.W. Walsingham, J. Chem. Soc. C, (1967) 2188; C.R. Bettler, J.C. Sendra and G. Urry, Inorg. Chem., 9 (1970) 1060; T.F. Schaaf, R.R. Kao and J.P. Oliver, Inorg. Chem., 14 (1975) 2288; G.A. Marano and A.G. MacDiarmid, Inorg. Nucl. Chem. Lett., 5 (1969) 621.

3 A.K. Hovland, T.F. Schaaf and J.P. Oliver, J. Organometal. Chem., 120 (1976) 171.

4 W.H. Ilsley, M.J. Albright, T.J. Anderson, M.D. Glick and J.P. Oliver, submitted.

5 R. Hoffmann and W.N. Lipscomb, J. Chem. Phys., 36 (1962) 2179.

6 R. Hoffmann, J. Chem. Phys., 39 (1963) 1397.

7 H. Basch, A. Viste and H.B. Gray, J. Chem. Phys., 44 (1966) 10.

8 H. Basch, Ph.D. Thesis, Columbia University, 1966.

9 R.D. Bach, J. Amer. Chem. Soc., 91 (1969) 1771.

10 M. Wolfsberg and L. Helmholz, J. Chem. Phys., 20 (1952) 837.

11 E. Clementi, Tables of Atomic Functions, supplement to paper in EBM, J. PCA (Portland Cem. Ass.) Res. Develop. Lab., 9 (1965) 2.

12 (a) P. Bleckmann, M. Soliman, K. Reuter and W.P. Neumann, J. Organometal. Chem., 108 (1976) C18; (b) W.H. Ilsley, E.A. Sadurski, T.F. Schaaf, M.J. Albright, T.J. Anderson, M.D. Glick and J.P. Oliver, J. Organometal. Chem., 190 (1980) 257.

13 L.S. Bartell, F.B. Clippard, Jr., and T.L. Boates, Inorg. Chem., 9 (1970) 2436.

14 Table of Interatomic Distances and Configuration in Molecular and Ions, London: The Chemical Society, Burlington House, WI, 1965.